ANKARA YILDIRIM BEYAZIT UNIVERSITY

GRADUATE SCHOOL OF NATURAL AND APPLIED SCIENCES



PRODUCTION AND CHARACTERIZATION OF ELECTROSPUN CHITOSAN/POLYPYRROLE NANOFIBERS AND INVESTIGATION OF THEIR ELECTROCHEMICAL PROPERTIES

M.Sc. Thesis by

Bedirhan BOZKURT

Department of Metallurgical and Materials Engineering

February, 2023

ANKARA

PRODUCTION AND CHARACTERIZATION OF ELECTROSPUN CHITOSAN/POLYPYRROLE NANOFIBERS AND INVESTIGATION OF THEIR ELECTROCHEMICAL PROPERTIES

A Thesis Submitted to
The Graduate School of Natural and Applied Sciences of
Ankara Yıldırım Beyazıt University
In Partial Fulfillment of Requirements for the Degree of Master of Science
in Materials Engineering, Department of Metallurgy and Materials Engineering

by

Bedirhan BOZKURT

February, 2023

Ankara

MSC THESIS EXAMINATION RESULT FORM

We have read the thesis entitled "**PRODUCTION AND CHARACTERIZATION OF ELECTROSPUN CHITOSAN/POLYPYRROLE NANOFIBERS AND INVESTIGATION OF THEIR ELECTROCHEMICAL PROPERTIES**" completed by **BEDIRHAN BOZKURT** under supervision of **ASSOC. PROF. DR. ŞERİFE AKKOYUN** and we certify that in our opinion it is fully adequate, in scope and in quality, as a thesis for the degree of Master of Science.

Assoc. Prof. Dr. Şerife AKKOYUN

Supervisor

Prof. Dr. Hüsnü Emrah ÜNALAN

Jury Member

Asst. Prof. Dr. Nimet Yıldırım TİRGİL

Jury Member

Prof. Dr. Sadettin ORHAN

Director

Graduate School of Natural and Applied Science

ETHICAL DECLARATION

I hereby declare that, in thesis which has been prepared in accordance with the Thesis Writing Manual of Graduate School of Natural and Applied Sciences,

- All data, information and documents are obtained in the framework of academic and ethical rules,
- All information, documents and assessments are presented in accordance with scientific ethics and morals,
- All the materials that have been utilized are fully cited and referenced,
- No change has been made on the utilized materials
- All the works presented are original,

and in any contrary case of above statements, I accept to renounce all my legal rights.

Date: …/…/2023 **Signature:**

Name & Surname: Bedirhan Bozkurt

ACKNOWLEDGMENTS

I sincerely thank my supervisor, Assoc. Prof. Dr. Şerife AKKOYUN for her support and guidance through this study. Her knowledge and perseverance gave me a better understanding of working harder to achieve higher goals. I am deeply thankful to her for her time and the effort she dedicated, which helps me to complete this dissertation and for the overall development of my career.

I would like to thank Prof. Dr. Hüsnü Emrah ÜNALAN and Asst. Prof. Dr. Nimet Yıldırım TİRGİL for accepting to be in the examination committee of my thesis.

I also wanted to thank my family for supporting and trusting me throughout this tough journey. Especially my beloved sister who always stand by my side with every decision I made. I always sensed their presence even in the hardest moments of this journey. The completion of this study would not have been possible without them.

We also acknowledge The Scientific and Research Council of Turkey (TUBITAK) for its financial support in a part this project (Project Code - 122 M852).

2023, February

Bedirhan Bozkurt

PRODUCTION AND CHARACTERIZATION OF ELECTROSPUN CHITOSAN/POLYPYRROLE NANOFIBERS AND IVESTIGATION OF THEIR ELECTROCHEMICAL PROPERTIES

ABSTRACT

The production of nanofibers with continuous and homogeneous structure still needs to be explored compared to other nano-sized materials. The aim of this thesis was to produce chitosan/polypyrrole (CS/PPy) nanofibers via electrospinning and to investigate their electrochemical properties. For this purpose, the challenging step of the electrospinning of CS and PPy particles containing CS nanofibers was first addressed. Then, nanofibers were coated on graphite oxide (GO) papers and finally, the characterization of the CS/PPy nanofibers were performed. For this purpose, pyrrole was polymerized by chemical oxidative polymerization before electrospinning. Firstly, solutions of 7 wt.% of CS in trifluoroacetic acid (TFA) were prepared and electrospun. In order to electrospun CS/PPy nanofibers, various amounts of PPy (0.2, 0.5, 1, 1.5, 2, 4, 6 and 8 wt.% of CS) were added to CS solutions. All the solutions were electrospun at a high voltage of 30 kV, a flow rate of 0.1mL/h and a tip-to-collector distance of 15 cm. The morphology and diameters of the PPy particles and electrospun CS/PPy nanofibers were examined by scanning electron microscope (SEM). According to SEM micrographs, spherical shaped PPy particles were obtained. Cylindrical and homogeneous nanofibers were also observed from the SEM examinations. Electrochemical properties were investigated via cyclic voltammetry (CV), differential pulse voltammetry (DPV) and electrochemical impedance spectroscopy (EIS). The highest oxidation and reduction activities of electrolyte were observed for the CS/PPy1 (chitosan/polypyrrole electrode with 1 wt.% of PPy). For higher PPy contents, the electrodes become more resistive. The originality of the study resides in the use of a natural polymer, CS nanofibers combined with a conjugated polymer PPy. To our knowledge, CS/PPy nanofibers

have not been produced as nanofiber materials via electrospinning and their electrochemical properties have not been investigated before.

Keywords: electrospinning, nanofibers, chitosan, polypyrole, conjugated polymers.

ELEKTROEĞİRME YÖNTEMİYLE ÜRETİLEN KİTOSAN/POLİPİROL NANOLİFLERİNİN ÜRETİMİ VE ELEKTROKİMYASAL ÖZELLİKLERİNİN İNCELENMESİ

ÖZ

Diğer nano boyutlu malzemelere kıyasla, devamlı ve homojen nanoliflerin süperapasitör uygulamalarında kullanımı keşfedilmeye çok açıktır. Bu tezin amacı, elektroeğirme yöntemiyle kitosan/polipirol (CS/PPy) nanoliflerini üretmek ve bunların elektrokimyasal özelliklerini incelemektir. Bu amaçla ilk olarak, elektroeğirme ile CS çözeltisinin ve PPy tozu katkılı CS çözeltilerinin zorlu elektroeğirme işlemleri gerçekleştirilmiştir. Daha sonra kağıt-bazlı GO elektrotlarının üzerlerine elektroeğirme yöntemiyle CS/PPy nanolifleri kaplanmıştır ve elektrokimyasal testlere tabi tutulmuştur. Bu amaçlar doğrultusunda ilk olarak, pirol kimyasal oksidadif polimerizasyon yöntemiyle polimerize edilmiştir. Daha sonra ağırlıkça %7 CS çözeltileri hazırlanmıştır. Hazırlanan bu CS çözeltilerine çeşitli miktarlarda PPy (kitosanın ağırlının %0,2, 0,5, 1, 1,5, 2, 4, 6 ve 8'i) eklenmiştir. Bütün çözeltiler aynı elektroeğirme koşullarında üretilmiştir. Bu elektroeğirme koşulları şunlardır; uygulanan voltaj 30 kV, debi 0.1 mL/h ve iğne ucu ile toplayıcı arası mesafe 15 cm'dir. Üretilen nanoliflerin ve PPy parçacılarının morfolojik incelenmesi ve çap ölçümleri Taramalı Elektron Mikroskopuyla (SEM) incelenmiştir. SEM görüntülerine göre homojen ve devamlı nanolifler üretilmiştir. Ayrıca elde edilen PPy parçacıkları küresel şekilde olup literatür ile benzer şekilde çıkmıştır. CS/PPy elektrotlarının elektrokimyasal analizleri Döngüsel Voltametre (CV), Diferansiyel Darbe Voltametresi (DPV) ve Elektrokimyasal Impedans Spektroskopi (EIS) yöntemleriyle incelenmiştir. Elektrolitin en yüksek yükseltgenme ve indirgeme aktiviteleri, PPy'nin ağırlıkça %1'ini içeren CS/PPy1 elektrodunda gözlemlenmiştir. Daha yüksek PPy içeriklerinde ise elektrotlar daha dirençli hale gelmiştir. Çalışmanın özgünlüğü, konjuge bir polimer olan PPy ile birleştirilmiş doğal CS polimerinin nanolif olarak kullanılmasında yatmaktadır. Bildiğimiz kadarıyla, literatürde CS/PPy nanoliflerinin elektroeğitme yöntemiyle üretilmiş bir

çalışmaması olmakta birlikte bunların elektrokimyasal özelliklerini inceleyen bir çalışma bulunmamaktadır.

Anahtar sözcükler: elektroeğirme, nanolifler, kitosan, polipirol, konjüge polimerler.

CONTENTS

MSC THESIS EXAMINATION RESULT FORM ii
ETHICAL DECLARATION iii
ACKNOWLEDGMENTS iv
ABSTRACT v
ÖZ vii
NOMENCLATURE xi
LIST OF TABLES xiii
LIST OF FIGURES xiv
CHAPTER 1 - INTRODUCTION 1
1.1 Literature Review 1
1.1.1 Electrospinning 1
1.1.4 Electrospinning of Conductive Polymers 11
1.2 Aim of the Thesis 14
CHAPTER 2 - MATERIALS AND METHODS 15
2.1 Materials 15
2.2 PPy Synthesis 15
2.3 Electrospinning of CS/PPy Nanofibers 17
2.4 Preparation of CS/PPy-GO Paper-Based Electrodes 18
2.5 Characterizations 22
2.5.1 Scanning Electron Microscopy (SEM) 22
2.5.1 Fourier Transform Infrared Spectroscopy (FTIR) 22
2.5.2 Electrochemical Analysis 22

CHAPTER 3 - RESULTS AND DISCUSSION 24

3.1 Characterization of Polypyrrole 24

3.1.1 SEM Analysis of PPy Particles..... 24

3.1.2 Study of Fourier Transform Infrared Spectroscopy (FTIR) 27

3.2 Effect of PPy Content on the Morphology and Diameter of the Nanofibers ... 29

3.3 Electrochemical Analysis of CS/PPy-GO Paper Electrodes 33

3.3.1 Cyclic Voltammetry Analysis (CV) 33

3.3.2 Differential Pulse Voltammetry (DPV) 35

3.3.3 Electrochemical Impedance Spectroscopy (EIS)..... 36

CHAPTER 4 - CONCLUSIONS..... 39

4.1 Perspectives 40

REFERENCES..... 41

CURRICULUM VITAE..... 48

NOMENCLATURE

Abbreviations

Ag	Silver
CS	Chitosan
CS/PPy0	CS nanofibers without PPy
CS/PPy0.2	CS nanofibers without 0.2 wt. % PPy (% of CS)
CS/PPy0.5	CS nanofibers containing 0.5 wt. % PPy (% of CS)
CS/PPy1	CS nanofibers containing 1 wt. % PPy (% of CS)
CS/PPy1.5	CS nanofibers containing 1.5 wt. % PPy (% of CS)
CS/PPy2	CS nanofibers containing 2 wt. % PPy (% of CS)
CS/PPy4	CS nanofibers containing 4 wt. % PPy (% of CS)
CS/PPy6	CS nanofibers containing 6 wt. % PPy (% of CS)
CS/PPy8	CS nanofibers containing 8 wt. % PPy (% of CS)
cm	Centimeter
DBSA	Dodecyl benzene sulphonic acid
DMF	Dimethylformamide
$FeCl_3.6H_2O$	Iron (III) chloride hexahydrate
g	Gram
GO	Graphite Oxide
kV	Kilovoltage
L	Liter
m	Mass
mM	Milimole
mL	Mililiter

M	Molar
Mw	Molecular weight
nm	Nanometer
PPy	Polypyrrole
Pt	Platinum
TFA	Trifluoroacetic acid
V	Voltage
wt.	Weight
%	Percentage
µm	Micrometer

LIST OF TABLES

Table 1.1 List of dopants and conductivities of some common conductive polymers …...…….....13

Table 2.1 Compositions of the different samples……..…….....17

Table 3.1 Average diameters of CS and CS/PPy nanofibers……...…….30

Table 3.2 Charge transfer resistance R_{ct} values for each CS/PPy electrodes……38

LIST OF FIGURES

Figure 1.1 Schematic representation of an electrospinning setup ……..……...3

Figure 1.2 Picture of the formation of Taylor cone ….……..……...…….4

Figure 1.3 List of the different parameters that affect the electrospinning process……...…..5

Figure 1.4 SEM micrographs of electrospun PEO nanofibers from polymer solutions of different concentrations. The concentration of the solution increases from 2a to 2d..…….……..…….…..6

Figure 1.5 SEM micrographs illustrating the effect of the flow rate on the morphology of the ultrafine PSF (polysulfone) nanofibers electrospun from a 20 % PSF/DMAC (polysulfone/ N,N-dimethylacetamide) (solution at 10 kV. Flow rate = 0.40 ml h^{-1} (a, b) and 0.66 ml h^{-1} (c, d)…..…….…….……..…..……..8

Figure 1.6 Chemical structure of chitosan (CS)….. …. ……...…….……..10

Figure 1.7 Chemical structures of some common conjugated polymers……..12

Figure 2.1 Schematic representation of PPy synthesis……..……...16

Figure 2.2 Photgraph of the polypyrrole powder synthesized……...……...……16

Figure 2.3: Schematic representation of electrospinning of CS/PPy nanofibers.....18

Figure 2.4: Schematic illustration of GO paper electrodes……...…….…19

Figure 2.5: SEM image of the matte paper electrode after brush painting of GO powder……...…….20

Figure 2.6 Schematic illustration of CS/PPy-GO paper electrodes …….…….....20

Figure 2.7 Photograph of a) a conventional matte paper, b) GO brush painted paper and c) CS/PPy-GO paper electrode…….……...21

Figure 2.8 Photograph of a CS/PPy nanofiber mat layer on a GO paper…….…….21

Figure 3.1 SEM micrographs of synthesized PPy particles…….……..24

Figure 3.2 Schematic illustration of CS/PPy nanofibers……...25

Figure 3.3 SEM micrographs of entrapped PPy particles……..26

Figure 3.4 FTIR spectra of polypyrrole (PPy), chitosan (CS) and Chitosan/Polypyrrole (CS/PPy) nanofiber mats…….28

Figure 3.5 SEM micrographs and average diameter distributions of CS and CS/PPy nanofibers with various PPy contents (< 2wt. % of CS)…….....31

Figure 3.6 SEM micrographs and average diameter distributions of CS and CS/PPy nanofibers with various PPy contents (> 2wt. % of CS)……..…….…….32

Figure 3.7 CV graphs of GO and CS/PPy electrodes at a scan rate of 0.02 V/s. Inset shows the sharp decrease of CV graphs for electrodes containing low amounts of PPy (< 2wt. % of CS)……34

Figure 3.8 Differential Pulse Voltammograms (oxidation and reduction) of graphite oxide (GO) and CS/PPy-GO electrodes at a scan rate of 0.02 V/s……35

Figure 3.9 Nyquist plots for the graphite oxide (GO) and CS/PPy electrodes. Inset shows relatively high frequency region. ……..…….37

CHAPTER 1

INTRODUCTION

Polymer-based nanofibers have attracted a lot of attention from the research and industry communities as a significant class of materials. Polymer nanofibers with submicrometric (<1 μm) diameters have special features, such as a high specific surface area per unit mass, which made it possible to add functions to variety of uses, from energy storage to biomedicine [1] [2].

1.1 Literature Review

1.1.1 Electrospinning

The term ‘electrospinning’ was derived from ‘electrostatic spinning’. The fundamental idea of electrospinning dates back to more than 60 years. Formalas published the experimental setup for the production of polymer filaments by using electrostatic force from 1934 to 1944. There was also no commercial interest in this technique until the 1990s [3].

A large number of nanofiber fabrication methods have been reported in the literature including thermally induced phase separation, drawing and template synthesis. Among them, electrospinning is one of the most convenient and promising method [4].

Thermally induced phase separation is generally used to fabricate microporous membranes. The procedure of this technique is not complex. Firstly, the polymer of interest should be dissolved in a high boiling point solvent. Then, the solution is casted into the desired shape, for instance, hollow fiber, flat sheet. Afterwards, it is cooled in a controlled manner to induce a phase separation and the polymer precipitates. So, membrane is formed from a homogeneous solution by removing the thermal energy to induce phase separation [5].

Template synthesis is another approach to produce nanofibers. It uses a template or mold to obtain a preferential structure or material. DNA replication can be considered as template-based synthesis [6]. In the method developed by Feng et al. [7], the template is a metal oxide membrane with nano-scaled pores. A polymer melt is extruded from the porous membrane by applying a water pressure. The extrudate solidify when contacting with cold solution and nanofibers with controlled diameters are formed.

Concerning the drawing process, this technique can only be applied to viscoelastic materials that deform at high temperatures but remain in their solid form to hold up the developed stress during pulling. In a typical drawing, the requirements are a silicon dioxide (SiO_2) surface, a micromanipulator and a micropipette to produce nanofibers. However, this process could not be scaled-up further than laboratory scale [8].

1.1.1.1 Principle

Figure 1.1 presents a schematic of an electrospinning setup. The system is basically composed of a syringe, a grounded metallic counter electrode or collector and a high voltage power supply. The grounded collector can be a flat plate or a drum. This process requires a polymer soluble in a highly volatile solvent. The polymer solution is injected towards a grounded collector. A high voltage is applied on the metallic needle. Before the formation of a jet through the collector, a Taylor Cone is formed [9].

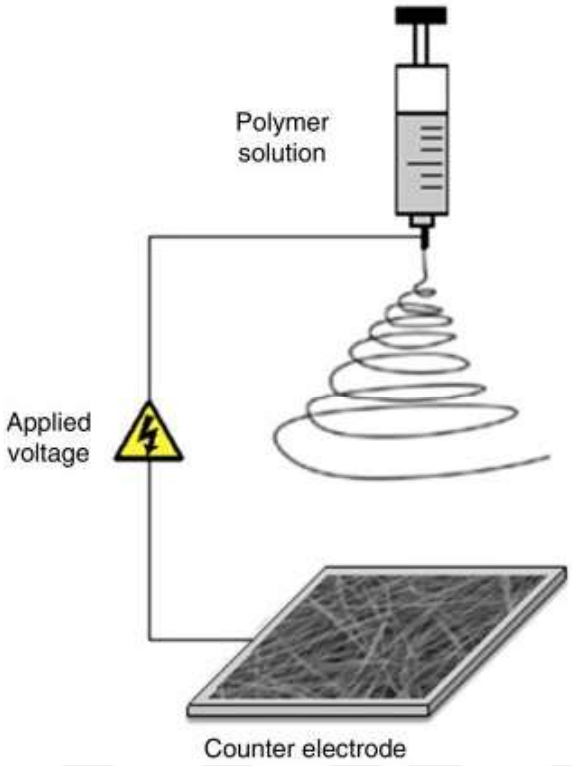


Figure 1.1 Schematic representation of an electrospinning setup [10].

Actually when a sufficiently high voltage is applied, the solution droplet at the tip of the needle becomes charged and electrostatic repulsion counteracts the surface tension. Then, the droplet is stretched and after a critical point, a stream of solution erupts from the surface of the droplet and if the molecular cohesion of the solution is high enough to break up the stream, a charged liquid jet is formed (Figure 1.2) [11].

When the Taylor Cone is formed and jet erupts from the surface of conical shaped structure, the solvent in the solution evaporates on its way to collector. Solid continuous nanofibers are gathered on the collector at the end of the process [12].

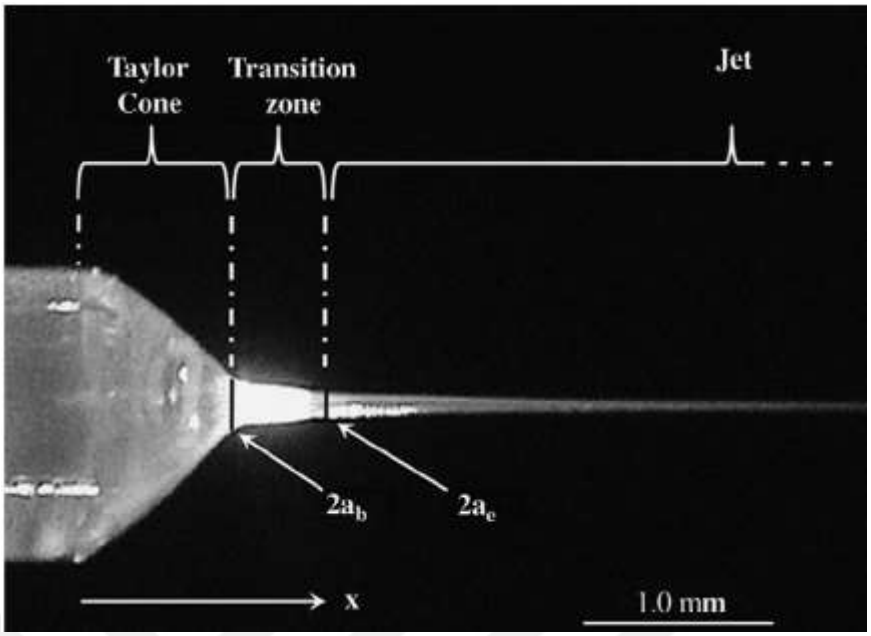


Figure 1.2 Picture of the formation of Taylor cone [13].

1.1.1.2 Parameters Affecting the Electrospinning Process

The production of nanofibers by electrospinning depends on many solution, processing and ambient parameters which affect the final nanofiber properties such as the diameter, homogeneity, continuity, porous structure or morphology.

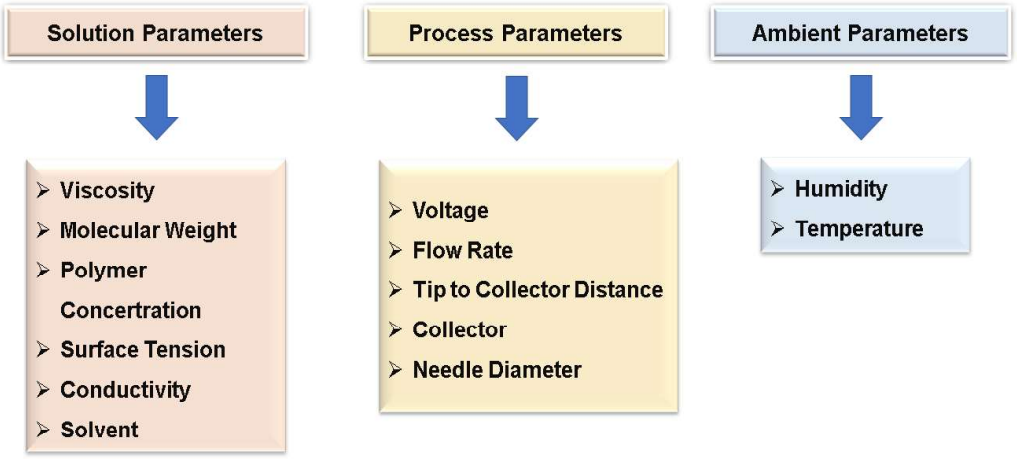


Figure 1.3 List of the different parameters that affect the electrospinning process.

An important solution parameter that affects the electrospinning process is the viscosity of the solution. This parameter strongly depends on the molecular weight of the polymer which determines the length of the polymer chain. Consequently, a solution of a polymer with a high molecular weight is more viscous than a solution of the same polymer with a low molecular weight. A polymer with a sufficient molecular weight is required for the production of nanofibers by electrospinning [14]. Another way to increase the viscosity of the polymer solution is obtained by increasing the polymer concentration in the polymer solution. Additionally, when the viscosity (and therefore the concentration of the solution) is excessively high, the solution may dry at the tip of the needle before electrospinning proceeds [15]. In the case of low viscosity and therefore low polymer concentration beaded nanofibers are obtained. When the polymer concentration increases, a gradual decrease on the number of beads is observed and the structure of the beads evolves from spherical to cylindrical [16] as shown in Figure 1.4.

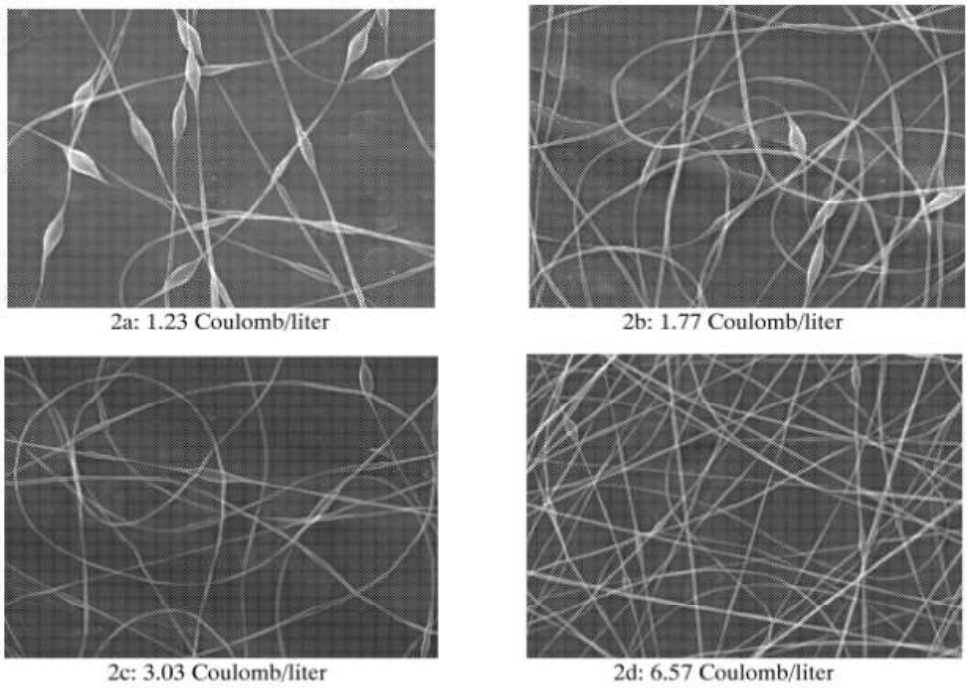


Figure 1.4 SEM micrographs of electrospun polyethylene oxide (PEO) nanofibers from polymer solutions of different concentrations. The polyethylene oxide (PEO) (8.4 wt. %, 9.1 wt. %, 10.3 wt. %, 11.5 wt. % and 12.5 wt. %) content increases in the solution from 2a to 2d [16].

Another parameter to consider for the electrospinning process is the surface tension of the polymer solution. When the surface charge of the polymer solution overcomes the surface tension, a solution jet is ejected from the tip of the needle through the metallic collector. When the surface tension of the solution is prevalent electrospraying occurs and droplets are formed on the collector. This process is different than the electrospinning and it is called as electrospraying.

The electrical conductivity of the polymer solution should also be taken into consideration. If it is high, more load would be applied for the formation of the jet. When small amounts of conductive material such as polyelectrolytes or ionic materials are added into the solution, they increase the charge carried by the solution. Hence the polymer solution stretches more. This also causes a decrease of fiber diameters [17]. The conductivity of the polymer solution can also be controlled by changing its pH. Low pH values induce an increase of the electrical conductivity of the polymer solution. Therefore, the nanofibers diameter is reduced [18].

During the electrospinning process, the solvent evaporates when the jet of the solution evolves through the collector. However, if the rate of evaporation of solvent is low, solid nanofibers cannot be gathered on the collector. Polymer chains are still dissolved into the solvent when the jet reaches the collector. The evaporation rate of the solvent is closely related to factors such as boiling point, surface tension, vapor pressure, entalphy, heat and the interaction between solvent soluble molecules [19].

The process parameters of electrospinning have also crucial effects on the production of nanofibers. As mentioned, the three main components of an electrospinning setup are a power supply, a syringe pump and a metallic collector.

The applied voltage induces an electric charge on the surface of the polymer solution. When the electrostatic forces overcome the surface tension of the solution, the fiber formation is initiated. At high voltages, the electric charge on the polymer solution causes nanofiber jet to accelerate faster to the collector. However, depending on the flow rate and the distance, high voltage values may not keep the Taylor Cone stable. Unstable form of Taylor cone is generally concluded as undesirable results on the formation of nanofibers. So, the applied voltage affects the tension of the polymer solution which also affect the morphology of the produced nanofibers [20].

Beaded form nanofibers have a potential to exist at higher voltages. Actually, higher voltages can raise the current instabilities. Therefore, the density of beads on the nanofibers can increase [18].

High voltages also favour the alignment of the polymer chains into the nanofibers which increases the degree of crystallinity. Undoubtedly, after a certain level, the voltage causes an increase of the fiber diameter.

The flow rate is also a process parameter that should be taken into consideration. In general, low flow rates are preferable compared to the higher flow rates as the polymer solution needs to get enough time to polarize and form a stable jet [21]. As shown in Figure 1.5, when the flow rate increases, the number of beads on the nanofibers and their diameter increase simultaneously. The optimal flow rate should give the solvent enough time to evaporate [22].

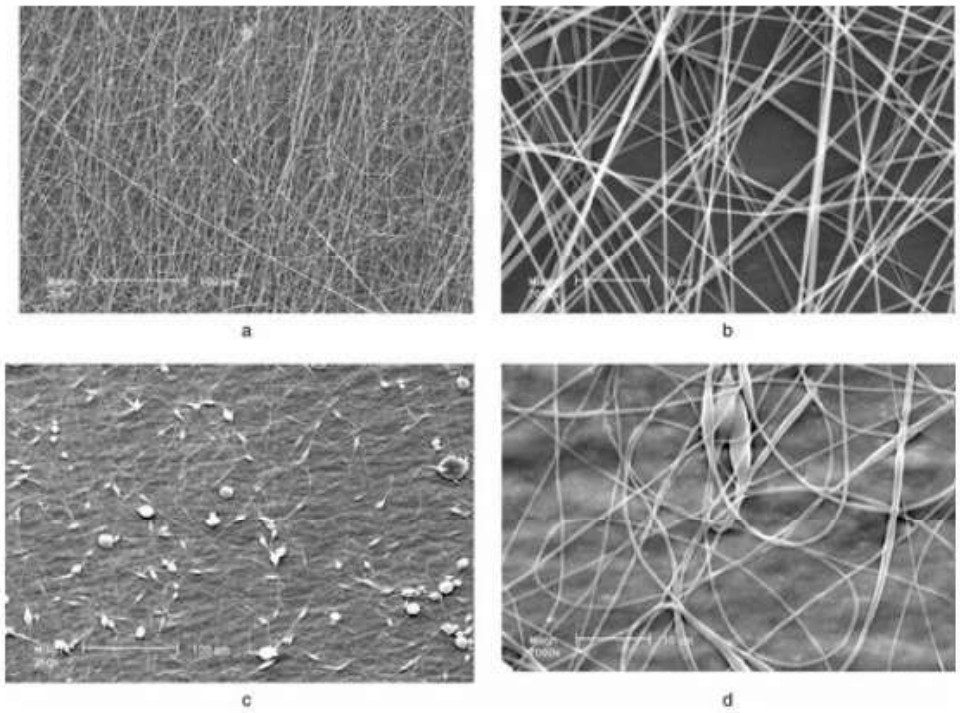


Figure 1.5 SEM micrographs showing the effect of the flow rate on the morphology of the ultrafine PSF (polysulfone) nanofibers electrospun from a 20 % PSF/DMAC (polysulfone/ N,N-dimethylacetamide) (solution at 10 kV. Flow rate = 0.40 ml h^{-1} (a, b) and 0.66 ml h^{-1} (c, d) [23].

The diameter of the needle has also an effect on the electrospinning process. Ibrahim et al. [24] showed that the smaller is the inner diameter of the needle, lower is the number of beaded nanofibers. The authors also showed that thin nanofibers obtained with thin needles.

Generally, an aluminium plate is used as grounded collector. In some cases, nonconductive materials are used as a sheet on the conductive plate. As expected, the accumulation of the nanofibers is less effective on these substrates [25]. Rotating drum collectors are used to produce aligned nanofibers. On the contrary, the nanofibers are randomly oriented on a flat collector [26].

Concerning the tip-to-collector distance, this parameter has a direct effect on the flight time of the jet and the electric field. If it is too short, the polymer jet has not enough time to solidify before reaching the collector surface. Additionally, the solvent which does not evaporate during the flight time may decomposer-dissolve the

polymer nanofibers. Increasing the tip-to-collector distance with an optimal high voltage induces fewer beads on the nanofibers because the electrostatic field between the tip of the needle and collector ensure enough tension for the flow [27]. Therefore, the average fiber diameters can decrease when the distance between the tip of the needle and collector increases.

Ambient parameters such as humidity and temperature have also considerable effects on the morphology and the diameter of the nanofibers. When the ambient temperature increases, the viscosity of the polymer solution decreases. This also tends to increase the evaporation rate of the polymer solution. Low viscosity solutions are 'stretched' easily compared to those with higher viscosities. Because, the tensile forces applied on the polymer solution increase, nanofibers with smaller diameters are obtained [28]. Concerning the humidity, its increase causes the formation of thicker nanofibers. [29]. Jeun et al. [30] showed that high humidity induces the formation of pores on the surface of electrospun poly(L-lactide-co-D, llactide) (PLDLA) nanofibers.

1.1.3 Electrospinning of CS Nanofibers

The production of bio-based macromolecular nanofibers are challenging due to their ionic character, ability to hydrogen bond and limited solubility in organic solvents. Chitosan is one of the natural polysaccharide biomaterials. It is a sustainable raw material which is originated from the N-deacetylated product of chitin [31]. Due to its low toxicity, biodegradability, and ecologically friendly behavior, the natural structure of chitosan has been shown with various application areas [32]. Besides these advantageous properties, chitosan has another important feature which is its ability to be processed as nanofibers, films or hydrogels. Chitosan nanofibers are classified as advanced bio-materials due to their properties [33].

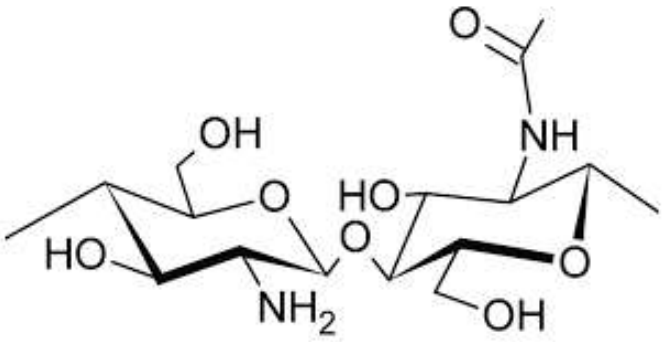


Figure 1.6 Chemical structure of chitosan (CS) [34].

The electrospinning process of chitosan is actually quite challenging. Its D-glucosamine repeat unit and high crystallinity make it difficult to dissolve in common solvents. The other difficulty is the hydrogen bonding ability which induces high intra and inter-molecular interactions. Therefore, chitosan solutions are too viscous which makes them difficult to electrospin. In addition, chitosan solutions have a polycationic character that increases the charge load on the polymer jet. Molecular weight, position of the acetylated groups and the deacetylation degree of chitosan varies due to the different chitin sources. These variations also influence the solubility of chitosan that makes it tough to create a general set of electrospinning parameters [35].

A few number of research groups have produced electrospun chitosan nanofibers. Okhawa et al. [36] is the first pioneer researcher succeeding in the electrospinning of chitosan (CS) nanofibers using trifluoroacetic acid as solvent. The authors mentioned that this was possible due to the interactions between trifluoroacetic acid (TFA) which allow to form a bulky salt and trifluoroacetic acid (TFA) disturbs the hydrogen bonding network between CS chains. Also the low boiling point of TFA is another advantage for electrospinning. In another study, the use of a trifluoroacetic acid/dichloromethane (TFA/DCM) solvent mixture was investigated to form nanofibers during the electrospinning [37]. When DCM was used as a co-solvent, the nanofiber diameter is getting narrower. Moreover, higher applied voltages cause a higher stretching of the nanofibers and as a consequence thinner nanofibers obtained.

TFA is not the only option to produce chitosan nanofibers. The high toxicity of TFA limits its use in a large scale production. In another study, chitosan nanofibers can be obtained from relatively less toxic solvent mixtures such as acetic acid/water [38]. The nanofibers are obtained from the electrospinning process due to the low deacetylation degree of chitosan (~ 60%) and high volume of acetic acid (90%). The authors have pointed out that the increase of the concentration of acetic acid from 10% to 90% induces a decrease of the surface tension which modifies the charge density of the solution. Increasing the net charge density affects the nanofibers smoothness due to the powerful whipping instability of the jet. The other important parameter which effects the electrospinning process is the viscosity of the solution. When the molecular weight of chitosan increases, its concentration in the solution must decrease in order to have a reasonable viscosity. In contrast, a lower molecular weight of CS causes the formation of beaded nanofibers [39].

1.1.4 Electrospinning of Conductive Polymers

Over the past decades, many studies focused on conductive polymers due to their outstanding properties like easy synthesis, wide range of controllable conductivity, lightweight attributes and corrosion resistance. These polymers have a structure showing the repetition of single and double bonds which is also named as conjugated structure. This unique property brings them electrical conductivity and high electron affinity. Conductive polymers are also classified as organic polymers class because of their tuneable properties [40].

Since the discovery of polyacetylene by Shirakawa, Heeger and MacDiarmid, metals and some inorganic crystalline structured materials were the only options for the electronic industry [41]. Other conjugated polymers were also synthesized and named as polypyrrole (PPy), polyaniline (PAN), poly(3 4-ethylenedioxythiophene), polythiophene (PT), poly (para-phenylene vinylene).

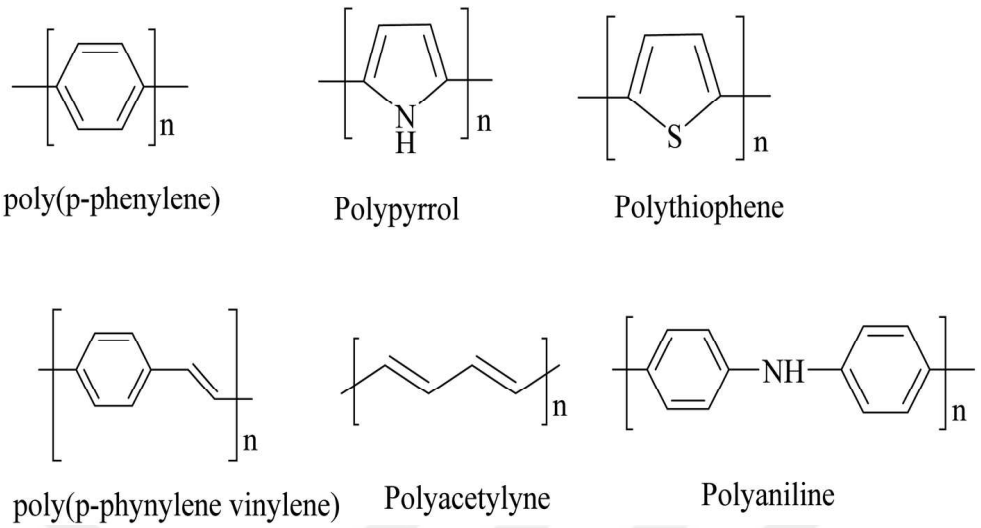


Figure 1.7 Chemical structures of some common conjugated polymers [42].

The backbone of conductive polymers consists of alternating single and double bonds. In the neutral state, they show the behaviour of insulative material. They become conductive after the doping process which can be chemical or electrochemical and consists of the addition or removal of electrons from the π system of the backbone. The formation of charge carriers occurs by applying oxidizing (p-doping) or reducing (n-doping) agents [42]. A list of conjugated polymers and corresponding dopants are given in Table 1.1.

Table 1.1 List of dopants and conductivities of some common conductive polymers [43].

Polymer	Dopants	Conductivity ($S.cm^{-1}$)
Polyacetylene	I_2, Br_2Li, Na, AsF_5	10^4
Polypyrrole	BF_4-, ClO_4-, tosylate	500-7.5 x 10^3
Polyaniline	HCl	200
Polyphenylene	AsF_5, Li, K	10^3
Polythiophene	BF_4-, ClO_4-, tosylate, $FeCl_4$-	10^3
Poly (phenylene vinylene)	AsF_5	2.7 x 103

Among conductive polymers, polypyrrole is one of the most attractive conductive polymer due to its high conductivity and low oxidation potential. In addition, it has been investigated in many applications such as electromagnetic shielding, batteries and actuators. The poor solubility of PPy in common solvents is one of the big disadvantage which restrict its practical application in some areas. [44] [45] [46].

Numerous attempts to produce PPy nanofibers by electrospinning exist. Kang et al. [46] have reported that PPy nanofibers were obtained using chloroform as solvent with an extra amount of dodecyl benzene sulphonic acid (DBSA) as dopant. The measured average diameter of the nanofibers and the conductivity values were 3 µm and 0.5 $S.cm^{-1}$, respectively. The authors have founded that the extra amount of dopant in the solution decreases intermolecular interactions. Therefore, the electrospinning process of PPy becomes easier. In another study, PPy particles were synthesized by chemical oxidative polymerization using iron (III) chloride $FeCl_3$ as

oxidant and dodecylbenzenesulfonic acid (DBSA) as dopant. The PPy particles obtained were added in a solution which contains polyvinylidene fluoride (PVDF) in dimethylformamide (DMF). The particles were dispersed in the solution by ultrasonication and the solution was electrospun. The resulting nanofibers obtained from the solution containing the highest amount of PPy (23 %) had an average diameter of 460 nm. In this study, the authors also investigated the piezoelectric behavior nanofibers obtained from PVDF/PPy solutions [47]. The same method was also applied to produce poly(acrylonitrile-co-vinyl acetate) nanofibers containing PPy particles in the same solvent [48]. In this study, the authors obtained lower average nanofiber diameter which was about 200-400 nm. However, the electrical conductivity value of nanofiber mats was 10^{-7} $S.cm^{-1}$. In that case, the low conductivity was related to the low amount of PPy content in the electrospinning solution

1.2 Aim of the Thesis

The aim of this thesis was to produce chitosan/polypyrrole (CS/PPy) nanofibers and to investigate their electrochemical properties. For this purpose, the challenging step of the electrospinning of CS and PPy particles containing CS nanofibers was first addressed. Then, nanofibers were coated on graphite oxide (GO) papers and finally, the characterization of the CS/PPy was performed. The originality of the study resides in the use of a natural polymer, CS nanofibers combined with a conjugated polymer, PPy. To our knowledge, CS/PPy nanofibers have not been produced by electrospinning and their electrochemical properties have not been investigated in the literature before.

CHAPTER 2

MATERIALS AND METHODS

2.1 Materials

Pyrrole (MW: 67.09 g/mol, density: 0.967 g/mL, 98 % purity), and Chitosan (CS - Low Molecular Weight) were purchased from Sigma Aldrich. TFA with a density of 1.49 $g.cm^{-3}$, Iron (III) chloride hexahydrate ($FeCl_3.6H_2O$) was purchased from Merck. Dodecyl benzene sulphonic acid (DBSA 70 % in isopropanol) (MW: 326.49 g/mol, d: 0.99 $g.mL^{-1}$) was purchased from the Sigma-Aldrich. Graphite powder (99 % purity) was supplied from Nanokar (D50 <1μm), ethanol with a density of 0.789 $g.cm^{-3}$ and MW: 46.07 $g.mol^{-1}$ was supplied from Dr Derman, Turkey (96 % purity).

2.2 PPy Synthesis

PPy was synthesized by the oxidative polymerization of Py according to the Merlini et al. [47]. In this process dodecyl benzene sulphonic acid (DBSA) is used as dopant and ferric chloride ($FeCl_3$) as oxidant. Before the polymerization, pyrrole was distilled to remove any residues. Then, DBSA (0.006 mol) was dissolved in 72 mL of DI water with pyrrole monomer 3 mL (0.3 $mol.L^{-1}$) for about 30 minutes. In the meantime, 23 g of Iron (III) chloride hexahydrate ($FeCl_3.6H_2O$) was completely dissolved in 72 mL of DI water. In the polymerization of pyrrole monomer, the ratio of oxidant to monomer was 2:1. The reaction was carried out for 6 hours at room temperature. Then, the precipitated black PPy particles were filtered and rinsed with an excess of DI water and ethanol until the residual solution under the Buchner was clear. A schematic description of the synthesis steps is provided in Figure 2.1.

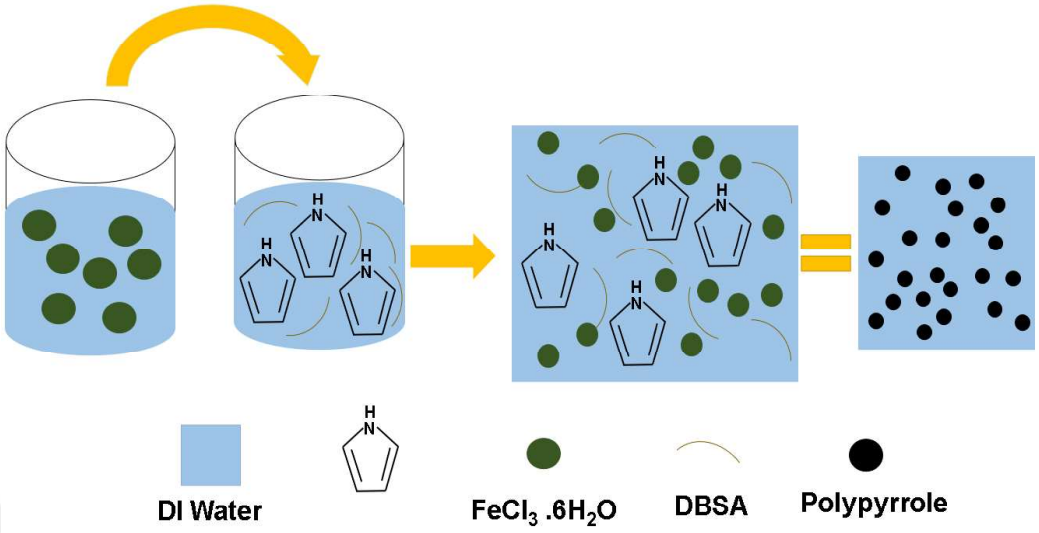


Figure 2.1 Schematic representation of PPy synthesis.



Figure 2.2 Photograph of the polypyrrole powder synthesized.

2.3 Electrospinning of CS/PPy Nanofibers

Solutions of 7 wt. % of CS in TFA were prepared a in sonication bath until the complete dissolution of CS. Then, different concentrations of PPy (0.2, 0.5, 1, 1.5, 2, 4, 6 and 8 wt. % of the CS) were added into the CS/TFA solutions with an excess of DBSA for a homogeneous dispersion of PPy particles by ultrasonication. The compositions of the different samples prepared are given in Table 2.1.

Afterwards, CS and CS/PPy nanofibers were electrospun using previously optimized process parameters (voltage: 30 kV, flow rate: 0.1 $mL.h^{-1}$ and tip-to collector distance: 15 cm). A schematic representation of the process is presented on Figure 2.3.

Table 2.1 Compositions of the different samples.

Samples	CS Concentrations (wt. %in TFA)	PPy Concentration (wt. % of CS)
CS/PPy0.2	7	0.2
CS/PPy0.5		0.5
CS/PPy1		1
CS/PPy1.5		1.5
CS/PPy2		2
CS/PPy4		4
CS/PPy6		6
CS/PPy8		8

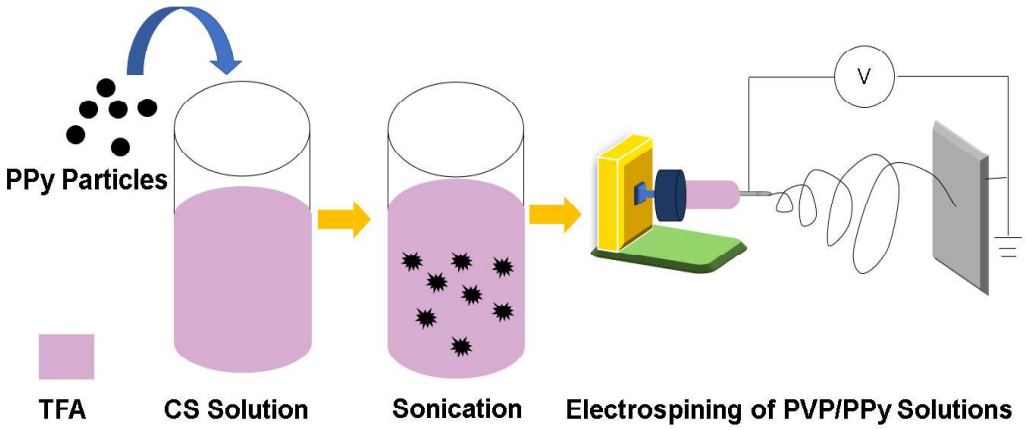


Figure 2.3: Schematic representation of electrospinning of CS/PPy nanofibers.

2.4 Preparation of CS/PPy-GO Paper-Based Electrodes

In a first step, the GO paper electrodes were prepared on a matte paper as schematically shown in Figure 2.4. This paper was chosen for its high stability in aqueous media due to its structured surface.

Then, the graphite powder was immersed in a highly acidic solution of sulphuric acid and nitric acid (H_2SO_4: HNO_3, 3:1) for five days. Then, the solution was filtered and rinsed with an excess of water until the pH was neutral. Afterwards, the acid treated graphite was dried in an oven overnight at 70°C. The dried GO powder was then ultrasonicated in the DMF to prepare a homogeneously dispersed slurry. Finally, the latter was brush painted on the paper substrates with dimensions of 10 x 10 cm^2. The SEM micrograph of the brush painted GO paper is shown in Figure 2.5.

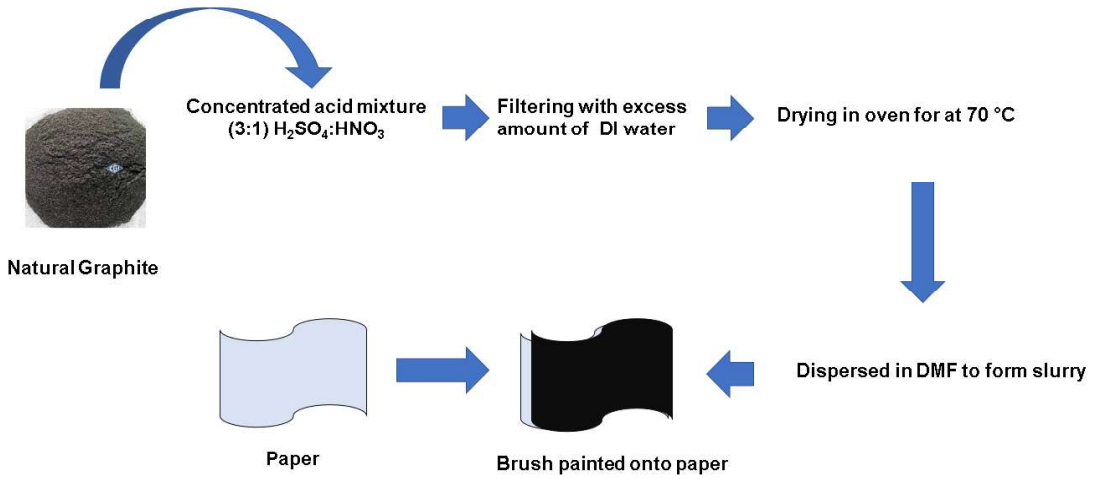


Figure 2.4: Schematic illustration of graphite oxide (GO) paper electrodes.

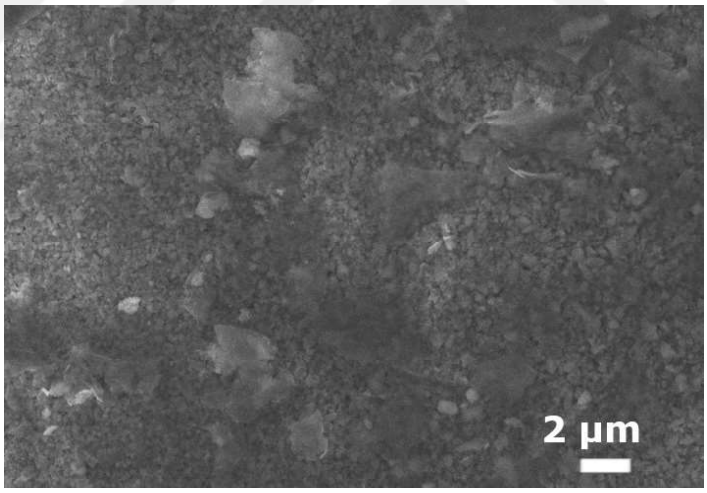


Figure 2.5: SEM image of the matte paper electrode after brush painting of graphite oxide (GO) powder.

In a next step, CS and CS/PPy nanofibers were electrospun onto the GO paper electrodes prepared. For this purpose, the GO papers were dried and placed onto the metallic collector of the electrospinning setup. Afterwards, the nanofibers were electrospun onto the papers as illustrated in Figure 2.6. Finally, the electrodes were cut into small pieces (1 x 2 cm^2) as can be seen in the Figure 2.7. The electrospun nanofiber mat layer is also shown in Figure 2.8.

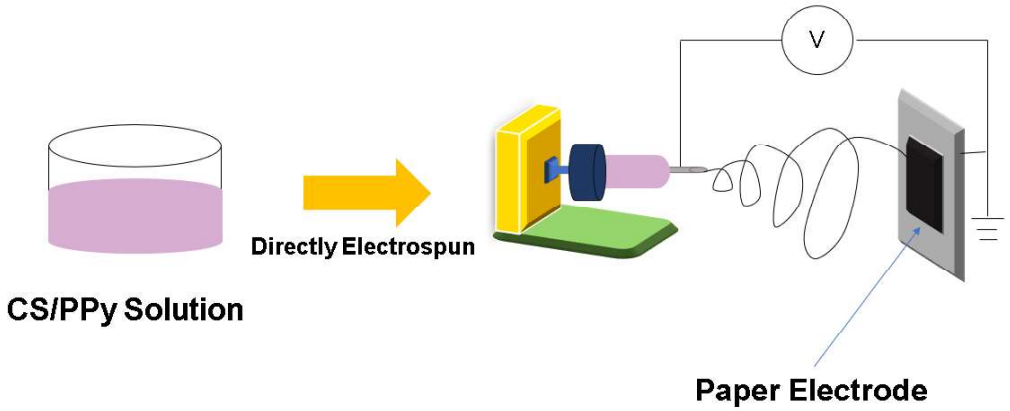


Figure 2.6 Schematic illustration of CS/PPy-GO paper electrodes.

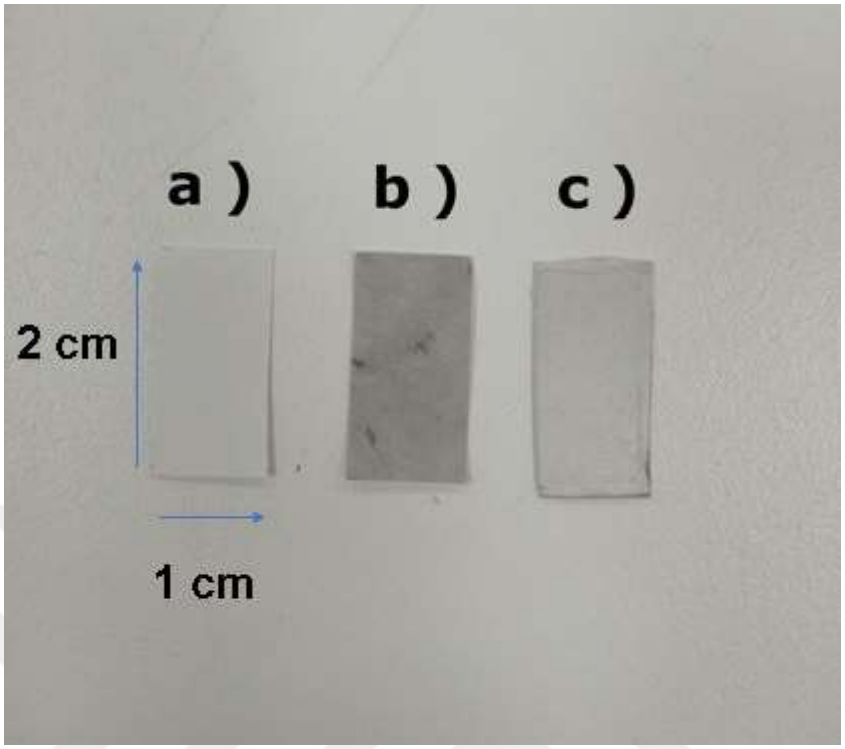


Figure 2.7 Photograph of a) a conventional matte paper, b) GO brush painted paper and c) CS/PPy-GO paper electrode.

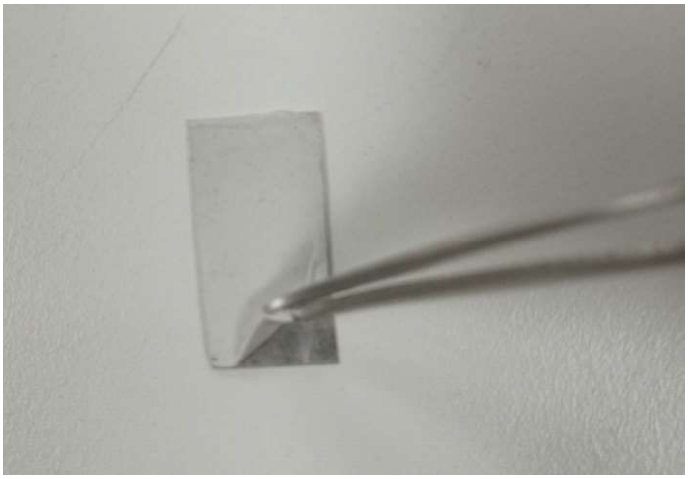


Figure 2.8 Photograph of a CS/PPy nanofiber mat layer on a GO paper.

2.5 Characterizations

2.5.1 Scanning Electron Microscopy (SEM)

Scanning electron microscopy (SEM, HITACHI Flex1000) at 15 kV was used to characterize the morphology and diameters of the electrospun nanofibers. The IMAGE J software (v.1.52i, National Institute of Health, USA) was used to determine the diameter of nanofibers from 100 nanofibers.

2.5.1 Fourier Transform Infrared Spectroscopy (FTIR)

Fourier transform Infra- Red (FTIR) spectrophotometer equipped with an attenuated total reflection (ATR) element. It is used to detect the polypyrrole (PPy) in/on the chitosan nanofibers.

2.5.2 Electrochemical Analysis

The electrochemical analysis of the CS/PPy-GO electrodes was performed using a CH600 potentiostat galvanostat electrochemical analyser/workstation. The analysis of the data was realized using a PSTRACE PalmSens Software. A 5 mM potassium ferricyanide ($K_3[Fe(CN)_6]$) solution containing 0.1M potassium chloride KCl was used as electrolyte. The main reason for choosing this electrolyte is that acidic or basic solutions harm the structure of CS/PPy nanofibers. All the measurements were conducted in a 10 mL conical beaker with defined electrode position.

2.5.2.1 Cyclic Voltammetry (CV)

The cyclic voltammetry measurements were realized with a three electrode configuration system in which Ag/AgCl was used as a reference electrode and Pt wire as a counter electrode. CV tests were scanned in potentials between -0.2 to 0.6 V at scan rate of 0.02 V/s for every electrode.

2.5.2.2 Differential Pulse Voltammetry (DPV)

The DPV measurements were made to investigate the movement of electrons of $K_3[Fe(CN)_6]$ on the working electrode which is in this study the CS/PPy-GO electrodes. The DPV measurements were also performed withing a potential range of -0.2 to 0.6 V at a scan rate of 0.02 V/s.

2.5.2.3 Electrochemical Impedance Spectroscopy (EIS)

EIS measurements were performed to record the charge transfer resistance of CS/PPy electrodes over a frequency range of 0.1 to 100000 Hz for each prepared electrode.

CHAPTER 3

RESULTS AND DISCUSSION

3.1 Characterization of Polypyrrole

3.1.1 SEM Analysis of PPy Particles

The morphological properties of PPy particles observed with SEM measurements are similar to the literature [49]. As can be seen from the Figure 3.1, spherical shaped PPy particles with average diameter of 113 nm were obtained.

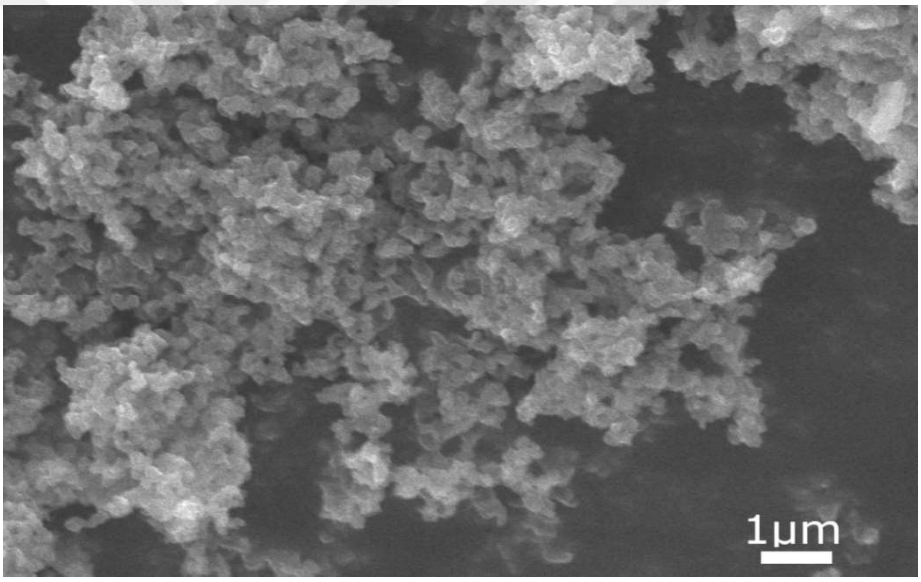


Figure 3.1 SEM micrographs of synthesized PPy particles.

After obtaining spherical shaped PPy particles, the intention is to produce CS/PPy nanofibers. For this purpose, it is desired to obtain PPy particles interior and exterior surface of the CS nanofibers. This intention is schematically illustrated in the Figure 3.2.

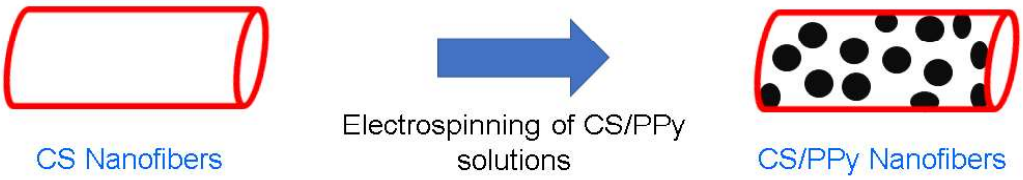


Figure 3.2 Schematic illustration of CS/PPy nanofibers.

Positions of PPy particles can be seen from Figure 3.3. All the SEM images of CS/PPy nanofibers did not appear transparent. Therefore, PPy particles in the CS nanofibers could not be observed. However, it can clearly be seen that PPy particles partially entrapped in the nanofibers. As can be seen from Figure 3.3, when the amount of PPy increased, more PPy particles can be observed on the nanofibers. Also, it is important to notice that when the PPy content increased, the homogeneity of nanofibers disturb.

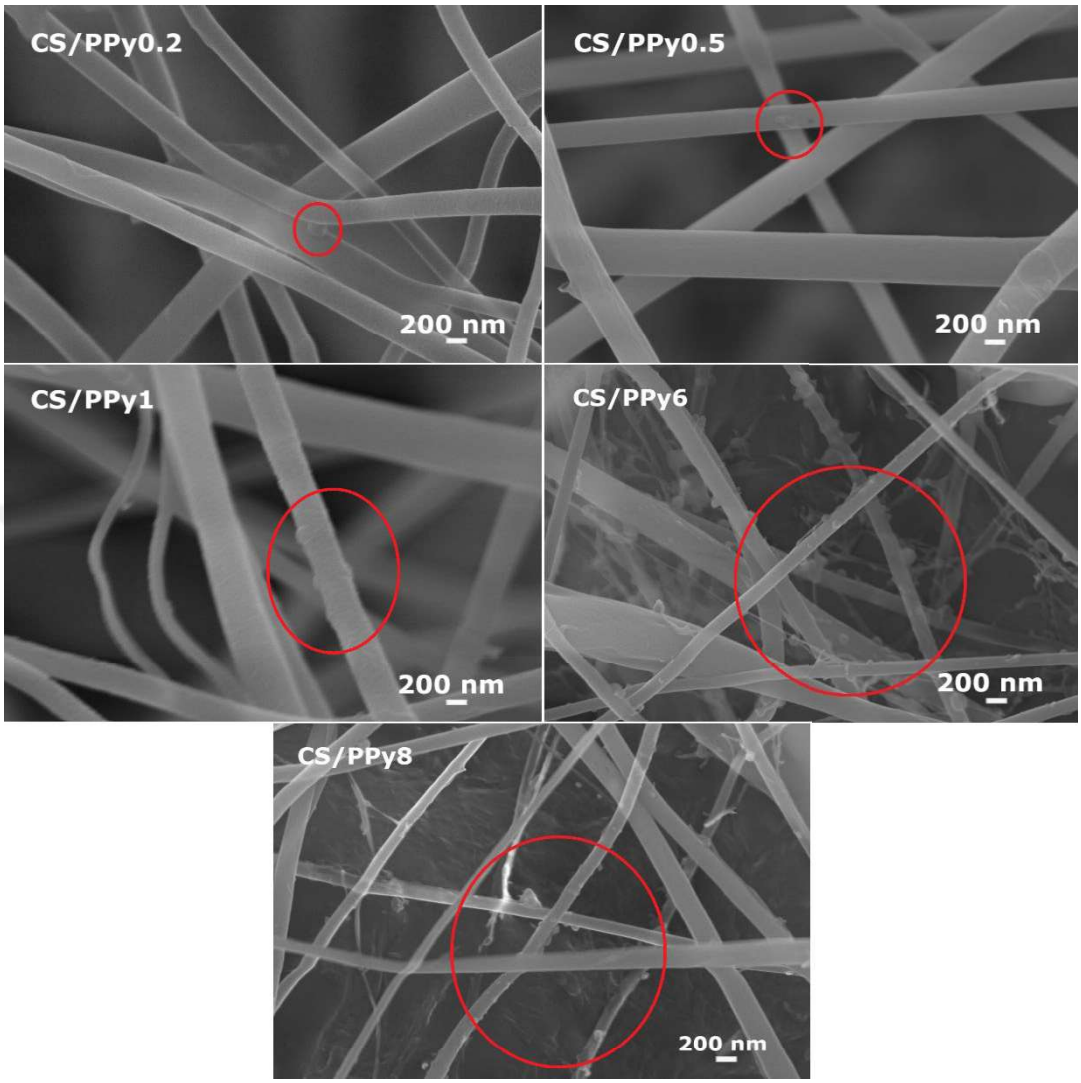


Figure 3.3 SEM micrographs of entrapped PPy particles.

3.1.2 Study of Fourier Transform Infrared Spectroscopy (FTIR)

PPy and CS/PPy nanofiber mat samples' FTIR spectra are shown in Figure 3.4. The PPy spectrum are very similar with the literature [47]. The bipolaron broad peaks at 910 and 1195 cm^{-1} show the existence of extended p-electron conjugation systems in the backbone of PPy. These doping-induced peaks show that PPy has been effectively doped [50]. Conjugation is also supported by the presence of two significant peaks at 1480 and 1550 cm^{-1}, which are caused by symmetric and antisymmetric ring stretching [51]. Therefore, PPy was successfully synthesized and doped. The bands at 1520 and 1425 cm^{-1} are attributed for the C-C and C-N stretching vibrations of the pyrrole ring. The in-plane deformation of C-H or C-N is attributed to the band at 1284 cm^{-1} [52]. The bands at 1125 and 1017 cm^{-1} represent the C-H bending mode, and the C-H out-of-plane deformation or C = C in-plane bending of the pyrrole ring is attributed to the peak at 956 cm^{-1}.

Infrared spectrum of CS is also similar to those described in the literature [53]. The band at 1736 cm^{-1} was assigned for C=O in the aldehyde on the terminal anhydro glucose unit [54]. Band found at 1392 and 1352 cm^{-1} is associated with C-O stretching vibration of CH_2-OH groups [55]. The band between 1240 and 1201 cm^{-1} represents the -C-O-C- bending mode. Also, the CH_2 bending and CH_3 symmetrical deformations were confirmed by the presence of bands at around 1240 and 1201 cm^{-1}, respectively [56]. Additionally, it was established that the band at 801 and 722 cm^{-1} corresponds to the C-O stretching. [57].

The FTIR spectra of CS/PPy nanofibers show absorption bands similar to those of neat CS. However, the noticeable shift can be realized at 910 and 1125 cm^{-1}. As can be seen from the Figure 3.4, the bipolaron peaks which indicates p-electron conjugation systems of PPy have shown its effect on the CS/PPy nanofibers.

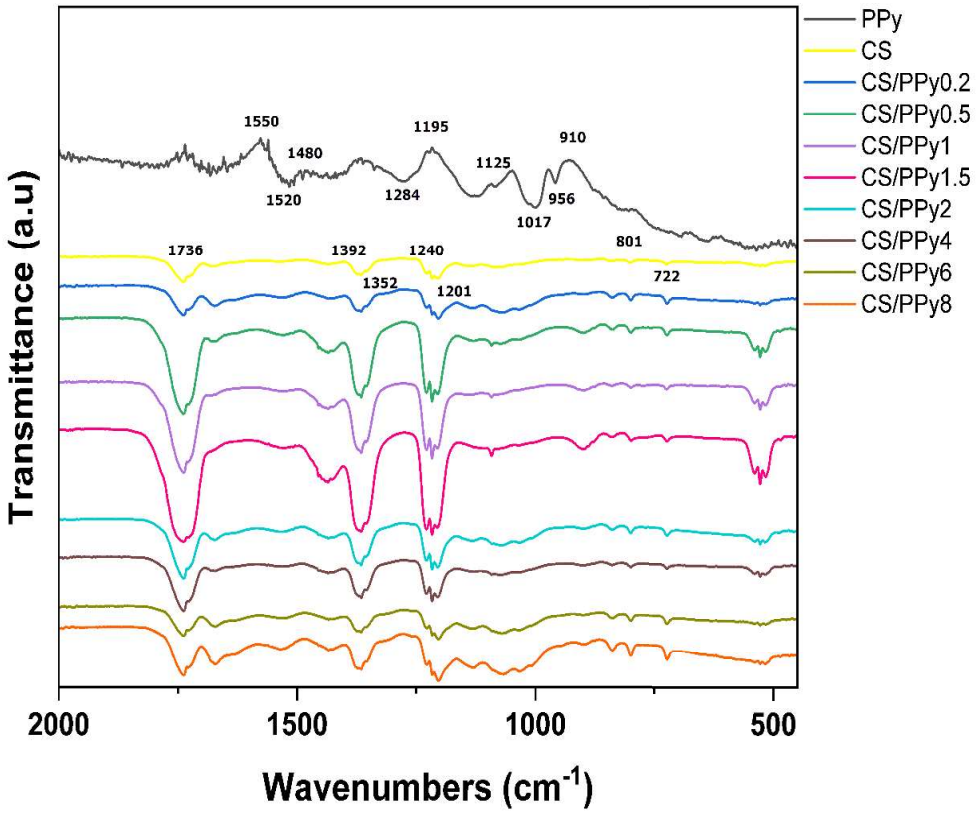


Figure 3.4 FTIR spectra of polypyrrole (PPy), chitosan (CS) and Chitosan/Polypyrrole (CS/PPy) nanofiber mats.

3.2 Effect of PPy Content on the Morphology and Diameter of the Nanofibers

The SEM micrographs of CS and CS/PPy nanofibers mats with low amounts of PPy (< 2 wt. % of CS) are shown in Figure 3.4 and those of samples with high amounts of PPy (≥ 2 wt. % of CS) are given in Figure 3.5. The corresponding average diameters are also gathered in Table 3.1. Figure 3.4 and Figure 3.5 show that all samples are constituted by a three-dimensional fibrous network. CS nanofiber mats without PPy display an average fiber diameter of 443 ± 40 nm. It is worthwhile to notice that the average diameter of CS/PPy nanofibers decreases when the PPy content increases until a value of 323 ± 57 nm for the CS/PPy8 sample. The addition of PPy into the polymer solution induces a modification of its properties such as the viscosity. As it can be seen from Table 3.1, when the amount of PPy increases from 0.2 to 8 wt. % (of CS), the average nanofiber diameter of each composition decreases gradually.

The diameter distributions presented in Figure 3.4 reveal that the distribution is narrower when the PPy content increases. The diameter distributions in Figure 3.5 follow the same behavior as those in Figure 3.4. The narrower distribution is observed when the PPy content is 2 wt. % which correspond to the case where the nanofibers have the most homogeneous structure. When the amount of PPy increases from 2 wt. % to 8 wt. %, the fiber diameter distribution becomes wider. The SEM micrographs show that the most homogeneous nanofibers are reached around a PPy content of 1 wt. %. The homogeneity is disturbed again for higher PPy amounts showing the presence of a critical amount of PPy.

Table 3.1 Average diameters of CS and CS/PPy nanofibers.

Nanofibers	Average Diameter (nm)
CS/PPy0	443 ± 40 nm
CS/PPy0.2	402 ± 68 nm
CS/PPy0.5	398 ± 51 nm
CS/PPy1	396 ± 39 nm
CS/PPy1.5	377 ± 54 nm
CS/PPy2	375 ± 59 nm
CS/PPy4	351 ± 64 nm
CS/PPy6	336 ± 73 nm
CS/PPy8	323 ± 96 nm

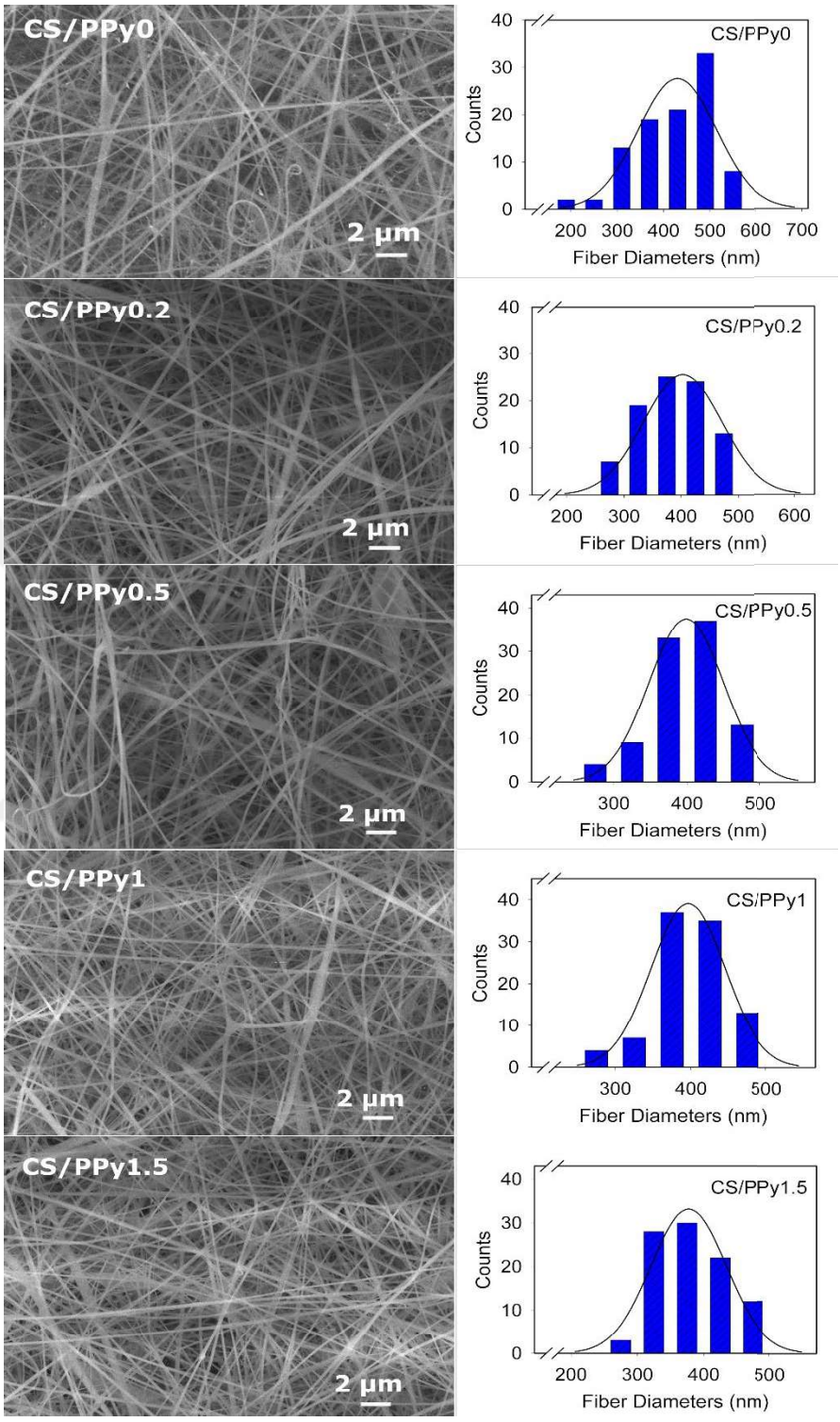


Figure 3.5 SEM micrographs and average diameter distributions of CS and CS/PPy nanofibers with various PPy contents (<2 wt. % of CS).